Available online at www.sciencedirect.com
ScienceDirect
European Polymer Journal 42 (2006) 2596–2605
EUROPEAN POLYMER JOURNAL
www.elsevier.com/locate/europolj

UV curable epoxy acrylate–clay nanocomposites

Fawn M. Uhl [a], Dean C. Webster [b,*], Siva Prashanth Davuluri [c], Shing-Chung Wong [c,1]

[a] *Center for Nanoscale Science and Engineering, North Dakota State University, 1805 NDSU Research Park Drive, Fargo, ND 58105, United States*
[b] *Department of Coatings and Polymeric Materials, North Dakota State University, 1735 NDSU Research Park Drive, P.O. Box 5376, Fargo, ND 58105, United States*
[c] *Department of Mechanical Engineering and Applied Mechanics, North Dakota State University, Dolve 111, P.O. Box 5285, Fargo, ND 58105, United States*

Received 27 January 2006; received in revised form 31 May 2006; accepted 15 June 2006
Available online 17 August 2006

Abstract

UV curable epoxy acrylates were reinforced with two different organically modified montmorillonites (MMTs) and an unmodified MMT. Conversion and rate of polymerization was monitored by real time infrared spectroscopy (RTIR) and photo-DSC. Microstructures were characterized by X-ray diffraction (XRD), transmission electron microscopy (TEM) and optical clarity. Optical clarity of the films containing clay was quite good as only a slight decrease was observed. Physical properties of the reinforced films were examined by differential scanning calorimetry (DSC), dynamic mechanical thermal analysis (DMTA), hardness and tensile testing. Enhancements in glass transition temperature (T_g), thermal stability and mechanical properties were observed. The films reinforced with the unmodified MMT exhibit the most significant enhancements in properties.

Keywords: Epoxy acrylate; UV curing; Clay nanocomposites

1. Introduction

Since the discovery by Toyota researchers that organically modified clay could be nanoscopically incorporated into a polymer matrix, research in this area has exploded and several review articles have been written on clay–polymer nanocomposites [1–3]. These articles review the preparation, structure and physical characterization of clay nanocomposites. Preparative methods include in-situ polymerization and melt blending. Structures observed include exfoliated morphology, where the clay layers are randomly dispersed within the polymer matrix and intercalated morphology, where there is an alternating structure of clay and polymer. In many cases a combination of the two morphologies can be observed. In general, an improvement or enhancement in many desirable polymer properties is noted for nanoreinforced polymers. These

* Corresponding author. Tel.: +1 701 231 8709; fax: +1 701 231 8439.
E-mail address: dean.webster@ndsu.edu (D.C. Webster).
[1] Present address: Department of Mechanical Engineering, The University of Akron, Akron, OH 44325, United States.

0014-3057/$ - see front matter © 2006 Elsevier Ltd. All rights reserved.
doi:10.1016/j.eurpolymj.2006.06.016

include increases in mechanical properties, barrier properties, thermal stability and chemical resistance at low loadings of clay [1–6].

While extensive research has been done on thermally initiated or melt blended nanocomposite systems less work has been done on UV curable polymer nanocomposites. UV curable films are being used in microelectronics devices as laminating and encapsulating polymers. There are several reasons industry is interested in these systems such as rapid cure, solvent free characteristics, application versatility, low energy requirements and low temperature operation [7,8]. Incorporation of nanoscopic particles into a UV curable system is expected to improve mechanical properties such as modulus, thermal and dimensional stability and barrier properties. There has been some initial work in examining UV curable polymer–clay nanocomposites by Zahouily et al. [9,10]. Decker et al. prepared UV curable polymer systems containing organomodified clay and suggested that an exfoliated structure was formed. The basis for this determination was due to the absence of an X-ray diffraction peak, slower sedimentation of the clay and a greater transparency for the nanocomposite versus microcomposite structures [11,12]. Decker has also shown an increase in tensile strength for polyurethane acrylate nanocomposites, but a decrease in elastic modulus and T_g by DMTA [11]. Benfarhi et al. examined various photocurable polymers – epoxide, vinyl ether and acrylate – with organically modified clays [13]. A decrease in T_g and increased flexibility and impact resistance for the nanostructure compared to the microstructure composite materials made with unmodified MMT was observed [13]. Wang et al. examined photopolymerization of methyl methacrylate and a *m*-cresol resin in the presence of organically modified montmorillonites [14]. They demonstrated that an intercalated structure is formed by photopolymerization as evidenced by XRD. This result is consistent with observations in our laboratory evidenced by both XRD and TEM [15–18].

Similar results have been observed and reported in our research group [15–18]. For UV curable urethane acrylate–clay nanocomposites, we have observed an increase in T_g and mechanical properties, an improvement in dimensional stability, etc. [15–18]. We have also examined the structures of these systems by TEM and shown that intercalated morphologies predominate [16].

We have previously examined UV curable urethane acrylate-organomodified clay formulations where we varied the ratio of oligomer to monomer and examined a variety of organomodified clays [15–19]. It is of interest to now start examining other types of UV curable matrix resins to determine if there is a more pronounced effect on structure and properties when the matrix structure is changed. In this paper we seek to examine the effect of clay nanoreinforcement on UV curable epoxy acrylate films. The structures formed using three different types of clay will be discussed as will the effect that each clay type has on the film properties.

2. Experimental

2.1. Materials

Nanomer I.31PS onium ion modified montmorillonite (ORG1) was supplied by Nanocor Inc. 15A Cloisite (ORG2) and Na^+ Cloisite (Na clay) were obtained from Southern Clay Products, Inc. The clays were used as received without further washing. CN121, a low viscosity aromatic epoxy acrylate oligomer with a functionality of two and SR454, an ethoxylated (3) trimethylolpropane triacrylate, were obtained from Sartomer. The photoinitiator, Darocur 1173, 2-hydroxy-2-methyl-1-phenylpropane-1-one, was obtained from Ciba Specialty Chemicals.

2.2. Preparation of nanocomposite polymer films

The formulation utilized in this study was a 1:1 mixture of CN121:SR454. The clay loadings in these systems were 1, 3 and 5 wt%. Clay–oligomer/monomer mixtures were sonicated for 8 h. Then the initiator Darocur 1173 (4 wt%) was added and the mixture stirred overnight. Films were cast onto glass, aluminum and polysulfone panels using a #1 Gardco casting bar with a gap of 4 mil.

2.3. Characterization

UV curing of samples was performed using a Dymax light source with a 200 EC silver lamp (UV-A, 365 nm). The intensity was 35 mW/cm^2 using a NIST Traceable Radiometer, International Light model IL1400A. Curing of samples was performed in air. X-ray powder diffraction (XRD) data were collected using a Phillips PW3040 X'pert-MPD Multipurpose Diffractometer in Bragg–Brentano geometry (CuK_α radiation). Qualitative variable slit data were collected over 2θ angles of 2°–40°, using a

step size of 0.02 and a run time of 1 s/step. TEM samples were cut using a diamond knife and RMC MTXL ultramicrotome. The ultrathin sections were then placed on 400 mesh copper grids and photographed using a JEOL 100cx-II Transmission Electron Microscope operating at 80 kV.

Fourier transform infrared (FTIR) was done using a Nicolet Magna-IR 850 Spectrometer Series II with detector type DTGS KBr. Scans were done in transmission mode from 4000 to 400 cm^{-1}. Photo-infrared was performed using the Nicolet Spectrometer and a UV optic fiber mounted in a sample chamber. Light source is a 100 W DC mercury vapor short-arc lamp. This setup monitors the conversion as reaction proceeds and is known as real time infrared spectrometry (RTIR). Samples were applied to a KBr disc by spin coating. Scans were taken over a 60 s period every 0.2 s and the UV source was adjusted to be approximately 14 mW/cm^2 at the sample. Measurements were performed both in air and nitrogen. From the initial portion of the RTIR plot (10 s or less), the rate of photopolymerization can be calculated. By following the absorbance of the =C–H out of plane band at 810 cm^{-1}, the degree of conversion and the rate of polymerization ($R_p/[M_0]$) can be calculated based on the following equations [20–22]:

Degree of conversion

$$= (((A_{810})_0 - (A_{810})_t)/(A_{810})_0) \times 100 \quad (1)$$

$$R_p/[M_0] = [((A_{810})_{t1} - (A_{810})_{t2})/(t_2 - t_1)] \quad (2)$$

where $(A_{810})_0$ is the absorbance before UV exposure, $(A_{810})_t$ is the absorbance at time t after UV exposure, $[M_0]$ is the initial concentration of acrylate double bonds and R_p is the rate of polymerization. The initial data points are used to calculate the rate of polymerization.

Differential scanning calorimetry (DSC) was performed using a TA Instruments Q1000 series calorimeter. Samples were subjected to a heat, cool, heat cycle from −20 to 200 °C at a ramp rate of 10 °C/min. T_gs were determined as the midpoint of the inflection from the 2nd heat cycle. Photo-DSC was performed utilizing the Q1000 DSC modified with the photocalorimic accessory (PCA) in a nitrogen atmosphere and the intensity was approximately 40 mW/cm^2. Sample sizes ranged from 4 to 6 mg. Reproducibility in photo-DSC has been found to be ±3%. Thermogravimetric analysis (TGA) was performed using a TA Instruments Q500 in air from ambient temperature to 1000 °C at a ramp rate of 20 °C/min.

Dynamic mechanical thermal analysis (DMTA) was performed using a Rheometric Scientific 3E apparatus in the rectangular tension/compression geometry. T_g is obtained from the maximum peak in the tan delta curves and crosslink densities are calculated from the E' value in the linear portion at least 50 °C greater than the T_g. Crosslink density can be calculated from the following equation [23]:

$$v_e = E/(3RT), \quad (3)$$

where v_e is the crosslink density. Sample sizes for mechanical testing were $(10 \times 5 \times (0.05–0.09))$ mm^3. The analysis was carried from −50 to 200 °C at a frequency of 10 rad/s and ramp rate of 5 °C/min. Tensile properties were measured using an Instron 5542; five specimens were taken for each sample to obtain an average value following ASTM D-2370. Test specimens for the tensile tests were free films with a length of 100 mm and grips were set to a distance of 40 mm. Width of samples was 5 mm and thickness of 0.05–0.09 mm. A crosshead speed of 20.0 mm/min was applied. Hardness tests were performed utilizing a BYK-Gardener pendulum hardness tester in the König mode in seconds. Samples for hardness testing were cured on an aluminum panel.

3. Results and discussion

3.1. Clay properties

3.1.1. X-ray diffraction (XRD)

In this study, three different clays were used. The first, called ORG1, is a commercially available clay from Nanocor with a d-spacing of 2.4 nm. The other two, ORG2 and Na clay are from Southern Clay Products Inc. ORG2 has a d-spacing of 3.1 nm and the Na clay, an unmodified montmorillonite (MMT), has a d-spacing of 1.1 nm. The organically modified MMTs differ in that ORG1 is modified using octadecylamine and γ-aminopropylethoxysilane as the organomodifiers [24], while ORG2 has a quaternary ammonium compound that contains two hydrogen tallow groups resulting in a much higher d-spacing [25–27]. The cation exchange capacities (CEC) of the MMTs used are ~145 meq/100 g and 92 meq/100 g for ORG1 and ORG2, respectively. For ORG2 the organomodifier concentration is reported to be 125 meq/100 g, indicating that there is an excess of organomodifier

present. The data for the organomodifier concentration for ORG1 is not available from the supplier.

3.1.2. Thermogravimetric analysis (TGA)

TGA in air was used to determine the amount of organomodifier and other volatile materials (e.g. water) in the clays. The ultimate weight loss of the clays was 35.2% for ORG1, 44.8% for ORG2 and 11.3% for Na clay. In the clay–polymer formulations, the clays were all added to the polymer system on a weight percent basis.

3.2. Structure of clay–polymer films

The clay–polymer films were examined for their morphology by both XRD and TEM. XRD shows that the peaks due to the ORG1 clay, *d*-spacing 2.41 nm, are absent in the nanocomposites at the 1 and 3 wt% loadings. It should be noted that absence of XRD peaks does not necessarily indicate exfoliation as extinguishment could be due to low clay concentration in the films and random orientation of clay tactoids. At the 5 wt% loading there is a peak observed at 1.9 nm which is lower than the original *d*-spacing of ORG1 suggesting that the d_{001} peak has shifted below 2θ. In the case of the ORG2 clay–polymer films, the same trend is exhibited; there are no peaks observed at the 1 and 3 wt% loadings, but a peak at 3.9 nm is observed in the case of the 5 wt% loading. For the unmodified MMT (Na clay), the 1 and 3 wt% loadings show a shift from 1.1 to 1.4 nm and the 5 wt% loading shows a shift to 1.3 nm. This increase in *d*-spacing may indicate that some of the low molecular weight oligomeric precursor has diffused into the clay layers. Transmission electron microscopy (TEM) was employed to further probe the structure of the clay–epoxy acrylate films. Fig. 1 shows the TEM micrographs of films modified with 3% clay. From this we can see that an intercalated morphology exists which is consistent with XRD data.

3.2.1. Optical clarity of clay–polymer films

The optical clarity of the films was good and was quantitatively assessed by UV–visible spectra shown in Fig. 2. (The sample strongly absorbs below 350 nm, so this portion of the spectrum is not shown.) The epoxy acrylate films are only slightly affected by the presence of the clay suggesting good dispersion and that the clay is indeed nanodispersed thus not significantly affecting the transparency of the films. We have previously examined polyester acrylate and urethane acrylate films containing the same clay [16,19]. Urethane acrylate films containing clay exhibit good transparency, similar to that of the epoxy acrylate system seen here. On the other hand, for polyester acrylate formulations, a more significant decrease in transmission is observed.

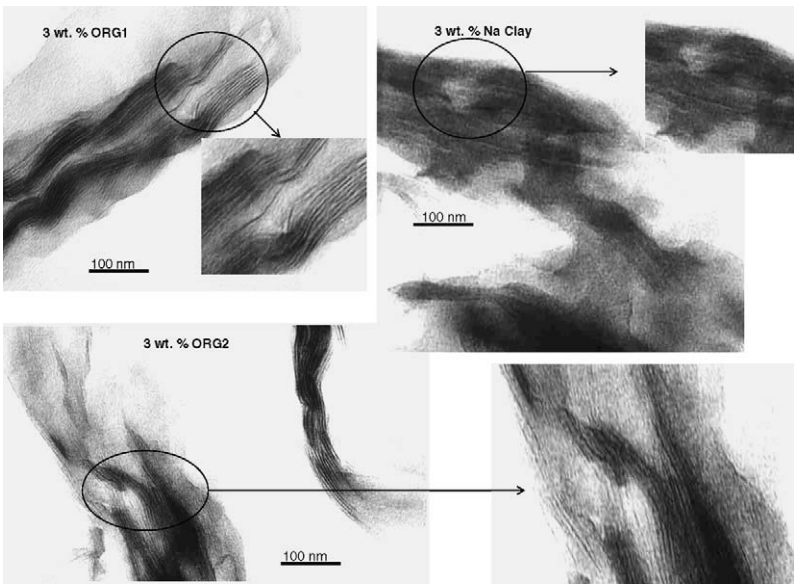

Fig. 1. TEM of epoxy acrylate films containing 3 wt% of the various montmorillonites. The dark regions are the clay layers dispersed in the polymer matrix. Higher magnification insets show that the clay sheets are oriented in layers, however, for the ORG1 and ORG2 systems the layers are spaced farther apart than for the Na clay sample.

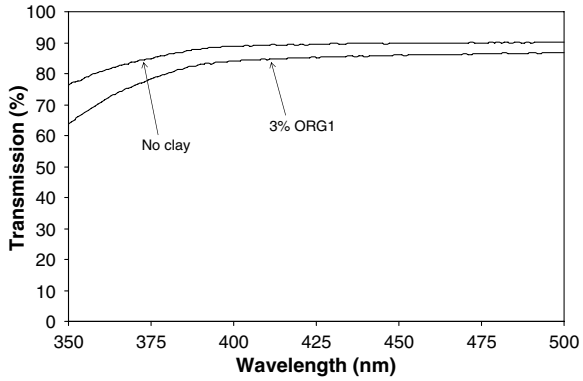

Fig. 2. UV–visible light transmission of films containing no clay and containing 3 wt% ORG1.

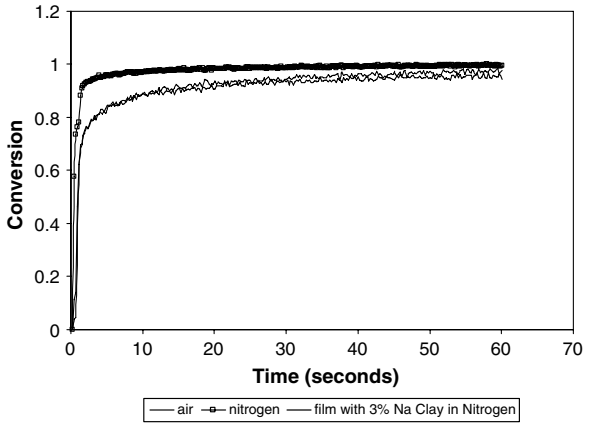

Fig. 3. RTIR plots of formulations with no clay in air and nitrogen and 3% Na clay in nitrogen.

That is, polyester acrylate formulations containing clay exhibits a lower optical transparency than either the urethane or epoxy acrylate formulations containing the organomodified clay. This likely indicates that the clay is better dispersed in the epoxy acrylate and urethane acrylate matrices than in the polyester acrylate and that the lower optical clarity is due to the strong scattering of the montmorillonite clay particles [28,29].

3.3. Clay–polymer film properties

3.3.1. Cure kinetics

During the curing process, the liquid acrylate functional polymer is rapidly converted to a tack-free film. Insight into the rate of cure and the effect of clay incorporation on the polymerization process can be gained using real-time Fourier Transform Infrared Spectroscopy (RTIR). In the RTIR experiments, the =C–H out of plane band at 810 cm^{-1} is monitored for determining acrylate conversion.

For this system, conversion at 60 s is quite high and very little difference between the clay–polymer films and the system containing no clay is seen. Also differences in conversion between air and nitrogen atmospheres are observed, as is typically seen in free radical systems. Fig. 3 shows plots of the RTIR data obtained for the film containing no clay in air and nitrogen atmospheres. The rate of polymerization is higher in the nitrogen atmosphere, due to the effect of oxygen inhibition for samples polymerized in air. For the formulation containing no clay, the R_p in the nitrogen atmosphere is 35% higher than that in air. In Fig. 3, the RTIR data for the film containing the Na clay polymerized in nitrogen is also shown. It is interesting that the polymerization rate and conversion of this sample is similar to that of the control film polymerized in air, indicating that the clay is interfering with the photopolymerization.

Comparison of the rate of polymerization for the films containing the clays, in air and nitrogen atmospheres, is shown in Fig. 4. For these formulations, a decrease in rate of polymerization is observed for all clay-modified samples regardless of the type of clay. The films containing ORG1 showed a decrease in R_p compared to the film containing no clay of ~40% at the 1 and 3 wt% loadings in air and a slight increase at the 5 wt%, in air, of 7%. In nitrogen, a decrease of 20–35% was observed. For the ORG2 containing films, a decrease of 10–60% in air and 20–40% in nitrogen was seen compared to the film

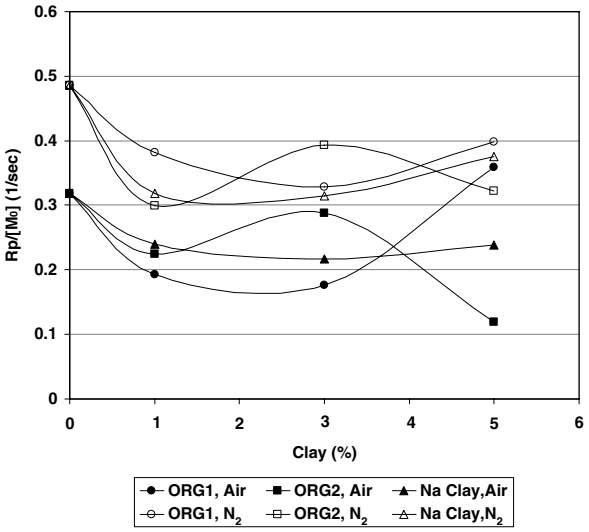

Fig. 4. Rate of polymerization from RTIR as a function of clay content in both air and nitrogen.

Table 1
Photo-DSC data for epoxy acrylate films

Sample	Clay (%)	H_{max} (W/J)	Area under curve (J/g)
Epoxy acrylate	0	66	339
ORG1	1%	67	285
	3%	62	296
	5%	54	319
ORG2	1%	58	259
	3%	54	268
	5%	51	237
Na clay	1%	60	281
	3%	64	268
	5%	60	250

containing no clay. For the Na clay films, a 20–35% decrease in R_p was seen in air and a 30–35% decrease in nitrogen.

Similar trends are seen in photo-DSC experiments, Table 1. ORG1 and ORG2 clay-films exhibit a decrease in H_{max} relative to the unmodified film. Also the decrease is dependent upon the amount of clay present. That is, as the amount of clay increases the H_{max} value decreases further. In the case of the Na clay, after the initial decrease there is no change in H_{max} regardless of the amount of Na clay present. The total area under the curve decreases upon the incorporation of clay into the films. The magnitude of the trends found in photo-DSC and RTIR are not exactly the same and this may be attributed to the higher light intensity used for the photo-DSC experiments compared to the RTIR experiments. However, both methods indicate that for the epoxy acrylate system, the presence of clay tends to deter the UV curing process.

These results are in contrast to our earlier work with urethane acrylate systems [16,18], as well as other work reported in the literature [30,31], where an enhancement in the rate of photopolymerization was seen in the presence of clay. In the previous studies, the increase in photopolymerization rate and conversion was attributed to a reduction in the termination rate due to immobilization of the reactive oligomer as a consequence of its high degree of interaction with the clay particles. In contrast, for this system, the reduction of the curing reaction may be due to one or a combination of two factors. First, the clay particles may be scattering the UV light, reducing the efficiency of the photoinitiation process. In addition, the fact that the curing is slower in the presence of the clay may indicate that the interaction of the clay with

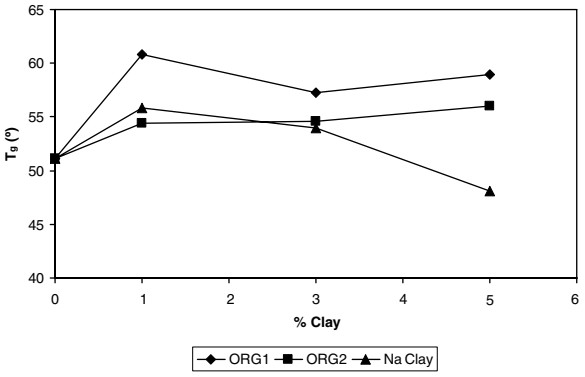

Fig. 5. T_g from DSC for the films containing the various clays.

the epoxy acrylate oligomer is not as strong as in the case of the urethane acrylate oligomer, thus the mobility of the system is not reduced and thus there is no reduction in the termination rate.

3.3.2. Thermal properties of clay–polymer films

3.3.2.1. Differential scanning calorimetry. Fig. 5 shows the T_g of the polymer films as a function of clay content. In the case of ORG1 films a significant increase in T_g is noted, up to 10 °C. The presence of nanoclays shifts the T_g to higher values as the polymer chain confinement effect is increased. With the ORG2 films an increase of 3–5 °C is observed and the Na clay films show an initial increase of 5 °C which then drops as the amount of clay is increased. This can be related to the uneven dispersion of the nanoclay in the epoxy acrylate, Fig. 1. ORG1 films appear to be better dispersed than the ORG2 and Na clay containing films.

3.3.2.2. Thermogravimetric analysis. Fig. 6 shows the TGA plots for the 5 wt% clay films and the film containing no clay. In the case of the ORG1 and Na

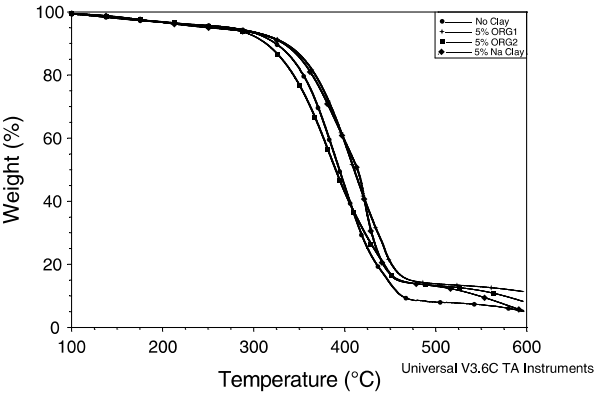

Fig. 6. TGA plots of 5 wt% clays in epoxy acrylate films.

clay films an increase in thermal stability compared to the control is observed while the ORG2 films exhibit a slight decrease in thermal stability. This is consistent with the TGA in air experiments for the organomodified clays where the ORG1 exhibited better thermal stability than ORG2. Thermal decomposition of organomodified clays generally begins with release of trapped water, followed by the decomposition of the organomodifier. Ammonium organomodifiers degrade via a Hoffman degradation mechanism and it has been shown that the clay can shift onset of decomposition to a lower temperature [32,33]. Using a similar organomodified clay as ORG2 in a polyamide matrix, Jang and Wilkie observed little change in thermal stability as a function of clay incorporation, similar to our result [34]. However, in experiments with a variety of polymer matrices containing ORG2-modified clay also modified with polycaprolactone, the thermal stability of the nanocomposite was enhanced [35]. Thus, the overall thermal stability can be affected by the organomodifier on the clay as well as the polymer matrix. This would suggest that a better interaction of the ORG1 modified clay with the epoxy acrylate is leading to these property enhancements. It is interesting that the Na clay nanocomposite also showed an improvement in thermal stability, indicating that the Na clay also interacts well with the epoxy acrylate.

3.3.3. Mechanical properties of clay–polymer films

3.3.3.1. Tensile properties. Mechanical property data is shown in Figs. 7–9. Young's Modulus shows an increase when clay is present in the epoxy acrylate films. An increase of 20–35% in Young's Modulus is seen for the ORG1 films while the ORG2 films show an increase of 10–20%. The Na clay films exhibit the most significant increase in Young's Modulus, ~50% and the increase is the same regardless of the amount of Na clay present. Similar trends are also seen in the tensile strength at break data. The only inconsistency is at the 1 wt% loading of the Na clay where only a 36% increase in tensile strength is seen. In general an improvement in elongation is also seen. This is especially true for the organically modified MMTs. In the case of the ORG1 films an increase of 6–20% in elongation is observed, while the ORG2 films show an increase of 10–20%. The Na clay films show an initial decrease in elongation at the 1 wt% loading and at the higher loadings an increase of 10–20% is observed. Unlike what we have previously observed for ORG1 in urethane acrylate formulations, an

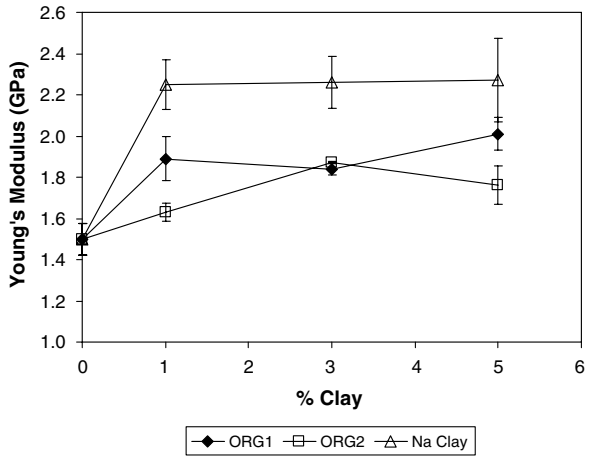

Fig. 7. Young's modulus for the epoxy acrylate films containing various clays.

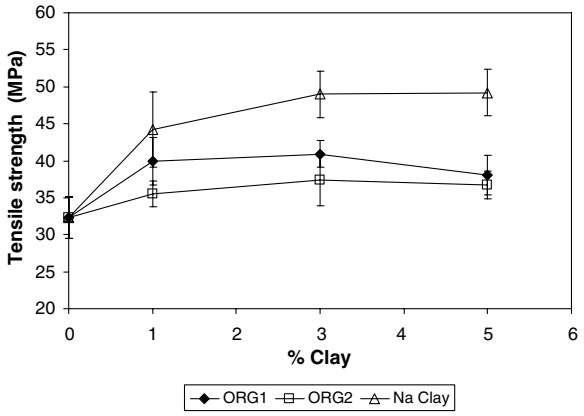

Fig. 8. Tensile strength for the films as a function of clay.

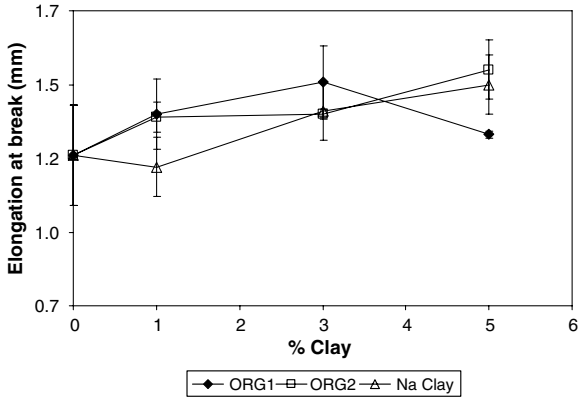

Fig. 9. Elongation at break versus clay content.

Table 2
Storage modulus (above and below T_g), T_g and crosslink density (XLD) from DMTA

Sample	Clay (%)	E' 25 °C (GPa)	T_g (°C)	E' 150 °C (GPa)	XLD (mol/cm^3)
Epoxy acrylate	0	2.2	89.0	0.064	6.0×10^{-3}
ORG1	1%	2.0	84.0	0.064	6.1×10^{-3}
	3%	2.4	84.1	0.071	6.7×10^{-3}
	5%	2.0	89.3	0.070	6.6×10^{-3}
ORG2	1%	2.4	89.0	0.073	6.8×10^{-3}
	3%	1.2	89.1	0.062	5.9×10^{-3}
	5%	2.4	89.1	0.077	7.3×10^{-3}
Na clay	1%	2.4	89.2	0.070	6.6×10^{-3}
	3%	2.7	93.8	0.082	7.7×10^{-3}
	5%	2.6	94.6	0.086	8.1×10^{-3}

increase in all three properties is observed: Young's Modulus, tensile strength and elongation [16]. The enhancement of the mechanical properties are attributed to the interaction of the epoxy acrylate matrix and the clay on a nanoscopic level.

3.3.3.2. Dynamic mechanical analysis. Films containing Na clay appear to have the most significant enhancement in properties by DMTA, Table 2. Storage modulus exhibits an increase both above and below T_g; 9–34% above T_g and 10–21% below T_g. Crosslink density also showed an increase of 10–35% for the samples containing Na clay as the nano-reinforcement. Organically modified clay films behaved slightly different than the Na clay films. ORG1 reinforced films had an increase in storage modulus above T_g and a slight increase in crosslink density as the amount of clay is increased. Storage modulus below T_g is more variable as the 3 wt% loading exhibited an increase in storage modulus relative to the unmodified film. In the case of the 1 and 5 wt% loadings a slight decrease in storage modulus and T_g is observed for these nano-reinforced films. In the case of the 1 and 5 wt% ORG2 reinforced films an increase in storage modulus, above and below T_g and an increase in crosslink density is observed. The 3 wt% loading of ORG2 in the epoxy acrylate films exhibit a decrease in storage modulus and crosslink density.

Interestingly, the films containing clay had an increase in measured crosslink density even though conversion and rate of polymerization, by RTIR, was lower for these films than the unmodified film. The increase in crosslink density can be related to the presence of clay. It is well known that polymer chains can physically aggregate onto particulate surfaces resulting in an increase in the effective degree of crosslinking [36]. Based upon our results, the clay acting as a crosslink due to interaction of the polymer with the clay surfaces is most likely what is being observed.

3.3.3.3. Hardness. König hardness values are highest for the films containing the Na clay and increases as the amount of clay is increased, Fig. 10. At the 1 wt% loading of ORG1 clay there appears to be no effect on hardness but as the amount of clay is increased to 3 and 5 wt% a significant improvement is observed. Interestingly the ORG2 clay shows no enhancement on hardness of the film regardless of the amount of ORG2 clay present. This increase in hardness is consistent with the increase in crosslink density and mechanical properties observed for these films.

3.4. Effect of Na clay

In this study, we have consistently observed that the unmodified pristine clay (Na clay) yields property enhancements similar to that observed using the organomodified clays. In some cases, the property enhancement is greater for the films containing the pristine clay than the organomodified clays (Young's modulus, tensile strength, hardness). Generally, it is believed that unmodified clays form conventional microcomposites when used with polymer matrices and that nanocomposites can only be formed when organomodified clays are used. A recent study by Jang et al. evaluated the effect of solubility parameter of organic clay modifications and polymer matrix resins on the morphology of the nanocomposite obtained [37]. They showed that nanocomposites having delaminated morphology can be prepared

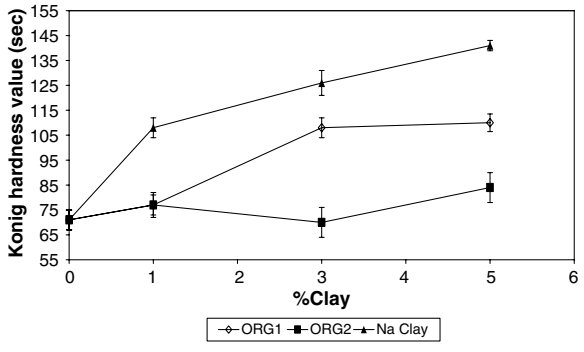

Fig. 10. Hardness values for the various clays in epoxy acrylate films.

from pristine clay and highly polar polymers using in-situ polymerization. Since the photopolymerizable precursors are highly polar and, since we see some evidence of interaction between the Na clay in the XRD data, and we observe enhancement of performance properties, the evidence leads us to the conclusion that an intercalated nanocomposite has been formed in this system.

3.5. Comparison with urethane acrylate and polyester acrylate systems

We have now explored the use of organically modified clays in three different UV curable systems: urethane acrylate [15–18], polyester acrylate [19] and now epoxy acrylate in this work. For all of the systems, it appears that intercalated nanocomposites are formed. That is, the organization of the clay tactoids is not completely disrupted during the process of blending the organomodified clay with the acrylated oligomers. In the urethane–acrylate systems, we have observed an enhancement in the rate of photopolymerization and conversion, while for the epoxy acrylate system, there is a decrease in the photopolymerization rate. Optical clarity of the coating films is generally good, with the exception of the polyester acrylate, indicating that the clay is dispersed well. In most systems, we observe an improvement in tensile modulus, tensile strength and glass transition temperature indicating that the clay is having a reinforcing effect. In the epoxy acrylate system we also observe a consistent improvement in the elongation at break, indicating that there is a high degree of interaction between the epoxy acrylate polymer and the clay. Thus, in all of these systems, there is clear indication that there is significant interaction of the clay with the polymer matrix leading to a reinforcing effect.

4. Conclusions

Structure and properties of UV curable epoxy acrylate films reinforced with nanoclay were studied. By XRD and TEM it is apparent that intercalated structures are formed and this is consistent with structures observed for previous studies of urethane acrylates reinforced with nanoclays [15–19]. Cure properties for the films containing clay as the nanoreinforcement are decreased relative to the film containing no clay. Also an increase in T_g, by DSC, for ORG1 and ORG2 modified MMTs is observed while an increase in thermal stability (by TGA) is seen for the ORG1 and Na clay MMTs. Mechanical properties are improved for all films containing MMT, both modified and unmodified. The Na clay reinforced films exhibited the most significant enhancement in mechanical properties including hardness. This is in contrast to what we have observed for the urethane acrylate films where the Na clay reinforced films exhibited the poorest properties [15–18]. This suggests that property enhancements are not only dependent upon the nanoclay but the structure of the polymer and how the two interact. So if a specific modified clay leads to property enhancements in one system, it may behave differently in another polymer system. It can be seen from the UV curable acrylate formulations we have studied that intercalated structures are formed and enhancements in properties are observed. Thus, the use of clay as a nanoreinforcement is a viable approach to improving the mechanical properties of UV curable films. These films may have use in applications such as electronic packaging materials for flexible electronic devices.

Acknowledgements

The authors thank the Center for Nanoscale Science and Engineering (CNSE) and the Defense Microelectronics Activity (DMEA), contract number DMEA-90-02-C-0224, for support of this research. One of us (SCW) acknowledges the support of NSF SGER Grant # CMS 0335390 on nanocomposites administered by the Mechanics and Materials Program.

References

[1] Ray SS, Okamoto M. Polymer/layered silicate nanocomposites: a review from preparation to processing. Prog Polym Sci 2003;28:1539–641.
[2] Ogawa M, Kuroda K. Preparation of inorganic–organic nanocomposites through intercalation of organoammonium ions into layered silicates. Bull Chem Soc Jpn 1997;70:2593–618.
[3] Alexandre M, Dubois P. Polymer-layered silicate nanocomposites: preparation, properties and uses of a new class of materials. Mater Sci Eng 2000;R28:1–63.
[4] Wang WJ, Chin W-K. Synthesis and structural characterizations of [chromophore]+-saponite/polyurethane nanocomposites. J Polym Sci Part B: Polym Phys 2002;40:1690–703.
[5] Tortora M, Gorrasi G, Vittoria V, Galli G, Ritrovati S, Chiellini E. Structural characterization and transport properties of organically modified montmorillonite/polyurethane nanocomposites. Polymer 2002;43:6147–57.

[6] Wu J, Lerner MM. Structural, thermal and electrical characterization of layered nanocomposites derived from Na-montmorillonite and polyethers. Chem Mater 1993;5: 835–8.
[7] Jackson P. Paint and Resin Times 2002;1:26–7.
[8] Fouassier JP. Photoinitiation, photopolymerization and photocuring fundamentals and applications. New York: Hanser Publishers; 1995. 246pp.
[9] Zahouily K, Benfarhi S, Bendaikha T, Baron J, Decker C. Proc RadTech Eur 2001:583–8.
[10] Zahouily K, Decker C, Benfarhi S, Baron J. A novel class of hybrid organic/clay UV-curable nanocomposite materials. Proc RadTech North Am 2002:309–20.
[11] Decker C. Photopolymer nanocomposites. Intl Symp on Polymer Nanocomposites, Vol. Montreal, 2003:37–43.
[12] Decker C, Zahouily K, Keller L, Benfarhi S, Bendaikha T, Baron J. Ultrafast synthesis of bentonite–acrylate nanocomposite materials by UV-radiation curing. J Mater Sci 2002;37:4831–8.
[13] Benfarhi S, Decker C, Keller L, Zahouily K. Synthesis of clay nanocomposite materials by light-induced crosslinking polymerization. Eur Polym J 2004;40:493–501.
[14] Wang H, Mei M, Jiang Y, Qingshan L, Zhang X, Wu S. A study on the preparation of polymer/montmorillonite nanocomposite materials by photo-polymerization. Polym Intl 2001;51:7–11.
[15] Uhl FM, Hinderliter BR, Davuluri SP, Croll SG, Wong S-C, Webster DC. UV curable montmorillonite–acrylate nanocomposites. Polymer Preprints 2003;44(2):247–8.
[16] Uhl FM, Davuluri SP, Wong S-C, Webster DC. Polymer films possessing nanoreinforcements via organically modified layered silicate. Chem Mater 2004;16:1135–42.
[17] Uhl FM, Hinderliter BR, Davuluri SP, Croll SG, Wong S-C, Webster DC. UV curable polymers with organically modified clay as the nanoreinforcements. Materials Research Society Symposium Proceedings, Vol. 788 (Continuous Nanophase and Nanostructured Materials). Boston, MA, 2003:203–8.
[18] Uhl FM, Davuluri SP, Wong S-C, Webster DC. Organically modified montmorillonite in UV curable urethane acrylate films. Polymer 2004;45:6175–87.
[19] Uhl FM, Hinderliter BR, Davuluri SP, Croll SG, Wong S-C, Webster DC. Enhanced properties of UV curable films containing layered silicates as the nanomaterial. In: Technical Conference Proceedings – UV & EB Technology Expo & Conference, Charlotte, NC, United States, May 2–5, 2004, p. 610–9.
[20] Stowe FS, Lieberman RA. Methoxy ether acrylates-novel radiation curing monomers. J Radiat Curing 1987;14:10–9.
[21] Decker C, Moussa K. A new method for monitoring ultra-fast photopolymerizations by real-time infra-red (RTIR) spectroscopy. Mackromol Chem 1988;189: 2381–94.
[22] Decker C, Moussa K. A new class of highly reactive acrylic monomers, 1 light-induced polymerization. Makromol Chem, Rapid Comm 1990;11:159–67.
[23] Wicks Jr ZW, Jones FN, Pappas SP. Organic coatings. 2nd ed. New York: John Wiley & Sons; 1999.
[24] Qian G, Lan T, Fay AM, Tomlin AS. Intercalates formed via coupling agent-reaction and onium ion-intercalation pretreatment of layered materials for polymer intercalation. US: Amcol Intl Corp; 2002.
[25] www.nanoclay.com/data/Na.htm [accessed January 2006].
[26] www.nanocor.com [accessed January 2006].
[27] www.nanoclay.com/data/15A.htm [accessed January 2006].
[28] Yeh J-M, Liou S-J, Lin C-Y, Cheng C-Y, Chang Y-W. Anticorrosively enhanced PMMA–clay nanocomposite materials with quaternary alkylphosphonium salt as an intercalating agent. Chem Mater 2002;14:154–61.
[29] Yu Y-H, Lin C-Y, Yeh J-M, Lin W-H. Preparation and properties of poly(vinyl alcohol)–clay nanocomposite materials. Polymer 2003;44:3553–60.
[30] Owusu-Adom K, Guymon CA. Photopolymerization of clay–polymer nanocomposite systems. PMSE Preprints 2005;92:374–5.
[31] Shemper BS, Morizur JF, Alirol M, Domenech A, Hulin V, Mathias LJ. Synthetic clay nanocomposite-based coatings prepared by UV-cure photopolymerization. J Appl Polym Sci 2004;93:1252–63.
[32] Xie W, Gao Z, Liu K, Pan WP, Vaia R, Hunter D, et al. Thermal characterization of organically modified montmorillonite. Thermochimica Acta 2001;367–368:339–50.
[33] Xie W, Gao Z, Pan W-P, Hunter D, Singh A, Vaia R. Thermal degradation chemistry of alkyl quaternary ammonium montmorillonite. Chem Mater 2001;13:2979–90.
[34] Jang BN, Wilkie CA. The effect of clay on the thermal degradation of polyamide 6 in polyamide 6/clay nanocomposites. Polymer 2005;46:3264–74.
[35] Zheng X, Wilkie CA. Nanocomposites based on poly(e-caprolactone) (PCL)/clay hybrid: polystyrene, high impact polystyrene, ABS, polypropylene and polyethylene. Polym Degrad Stabil 2003;82:441–50.
[36] Mark JE, Erman B. Rubberlike elasticity A molecular primer. New York: John Wiley & Sons; 1988. 145pp.
[37] Jang BN, Wang D, Wilkie CA. Relationship between the solubility parameter of polymers and the clay dispersion in polymer/clay nanocomposites and the role of the surfactant. Macromolecules 2005;38:6533–43.